Characterization and Distribution of Seagrass Habitats in a Caribbean Nature Reserve using High-Resolution Satellite Imagery and Field Sampling

Authors: León-Pérez, Mariana C., Hernández, William J., and Armstrong, Roy A.

Characterization and Distribution of Seagrass Habitats in a Caribbean Nature Reserve using High-Resolution Satellite Imagery and Field Sampling

Mariana C. León-Pérez[†‡*], William J. Hernández[§], and Roy A. Armstrong[†]

[†]Department of Marine Sciences
University of Puerto Rico–Mayagüez
Lajas 00680, Puerto Rico

[‡]Harte Research Institute for Gulf of Mexico Studies
Texas A&M University–Corpus Christi
Corpus Christi, TX 78412, U.S.A.

[§]NOAA CESSRST
City College
City University of New York
New York, NY 10031, U.S.A.

www.cerf-jcr.org

www.JCRonline.org

ABSTRACT

León-Pérez, M.C.; Hernández, W.J., and Armstrong, R.A., 2019. Characterization and distribution of seagrass habitats in a Caribbean nature reserve using high-resolution satellite imagery and field sampling. *Journal of Coastal Research,* 35(5), 937–947. Coconut Creek (Florida), ISSN 0749-0208.

Effective management of seagrass habitats requires detailed information about seagrass condition and distribution. This paper addresses the first step of a larger study to assess long-term changes in seagrass distribution within Caja de Muertos Island Nature Reserve, Puerto Rico. A high-spatial-resolution characterization of seagrass beds in the reserve was conducted using a WorldView-2 (WV-2) image and field data set. The WV-2–derived seafloor reflectance and bathymetry data were used to conduct an object-based image analysis (OBIA). The selection of bands for this analysis was based on *in situ* spectral water attenuation measurements. The resulting polygons of the OBIA were classified through a supervised classification and contextual editing. Calibration and validation of the image were conducted using 164 sampling sites. Together with traditional accuracy assessment tools, a reliability map was created to provide another metric for evaluating the map accuracy. Overall accuracy was 96.59%, and the total seagrass accuracy was 100%. Seagrass beds were found mainly west and north of the island and were mostly composed of a combination of *Thalassia testudinum* and *Syringodium filiforme*. Results suggested that light availability was not a limiting factor for seagrass colonization at the study area and that strong wave energy may be an important factor in regulating seagrass distribution. This seagrass habitat map improved upon previous mapping efforts and represents the first high-spatial-resolution map for the reserve. The data and methods used proved to be effective for mapping seagrass habitats within a highly complex benthic environment.

ADDITIONAL INDEX WORDS: *WorldView-2, benthic habitat mapping, seagrass distribution, clear shallow waters*.

INTRODUCTION

Seagrasses are some of the most valuable and productive shallow-water ecosystems in the ocean (Zieman and Zieman, 1989). Seagrass beds provide several important ecosystem services, such as nursery and feeding grounds for a diverse number of organisms, nutrient recycling, fisheries resources, sediment stabilization, and carbon sequestration from the atmosphere (Costanza *et al*., 1997; Duarte, 2002; Orth *et al*., 2006; Waycott *et al*., 2009; Zieman and Zieman, 1989).

The distribution of seagrass is determined by a series of physical factors such as temperature, light availability, currents and wave energy, substrate type, salinity, and turbidity (Gonzalez-Liboy, 1979; Miller and Lugo, 2009). The occurrence or absence of different seagrass species depends on the unique adaptations of each species and their tolerances to variability in these factors. Because of the high requirements of seagrass for adequate amounts of light, they are particularly affected by changes altering water clarity (Duarte, 2002; Orth *et al*., 2006).

Seagrass beds are vulnerable and subject to a wide range of natural and anthropogenic stressors, such as extreme weather events, predation, mechanical damage, increased turbidity, and eutrophication, among others (Duarte, 2002; Orth *et al*., 2006; Short and Wyllie-Echeverria, 1996). These ecosystems are declining worldwide, with major losses caused by human actions, particularly sediment runoff and increased nutrients (Orth *et al*., 2006). Therefore, it is important to conduct both baseline characterizations and monitoring of the condition and distribution of seagrass habitats.

Worldwide, passive remote-sensing data such as aerial photography (Armstrong, 1981; Hernández-Cruz, Purkis, and Riegl, 2006; Kendrick *et al*., 2002; Lathrop, Montesano, and Haag, 2006; Maccarrone, 2010; Moore *et al*., 2001; Yarbro and Carlson, 2015) and multispectral imagery (Hoang *et al*., 2016; Lyons, Phinn, and Roelfsema, 2011, 2012; Roelfsema *et al*., 2009) have been effectively used for mapping and monitoring shallow seagrass beds. The most commonly and recently used multispectral satellite data come from Landsat sensors (Armstrong, 1993; Lyons, Phinn, and Roelfsema, 2012; Roelf-

sema *et al.*, 2013), and WorldView 2 and 3 imagery (Hoang *et al.*, 2016; Koedsin *et al.*, 2016; Roelfsema *et al.*, 2014), although the last provides more detailed and representative information of seagrass distribution because of its higher spatial resolution (Kovacs *et al.*, 2018). To account for the variety of remote-sensing data, and mapping challenges in different environmental conditions, seagrass mapping techniques have evolved and adapted to specific local needs. For example, object-based image analysis (OBIA) has been recently used over traditional manual delineations and pixel-based classifications (Kågesten *et al.*, 2015; Lathrop, Montesano, and Haag, 2006; Lyons, Phinn, and Roelfsema, 2012; Roelfsema *et al.*, 2013, 2014, 2018; Wahidin *et al.*, 2015), because it extracts the spatial features of ecologic interest by incorporating the spectral signature, shape, and texture of benthic features (Veljanovski, Kanjir, and Ostir, 2011).

In Caja de Muertos Island Nature Reserve (CMINR), Puerto Rico, little is known about the status and dynamics of seagrass beds. Updated information about seagrass distribution and historical changes in the reserve will help decision makers understand and manage the resource more efficiently. The research presented here is the first part of a larger analysis to assess long-term changes (1950–2014) in seagrass distribution within the CMINR. The objective of this paper is to provide updated, high-spatial-resolution information about seagrass habitats in the reserve using remote-sensing and field data.

METHODS

The methods are presented in the following subsections: study area, image data acquisition and preprocessing, field data acquisition and analysis, classification approach, and accuracy assessment.

Study Area

CMINR in Puerto Rico contains approximately 57 km^2 of protected land and water area. This reserve is composed of Caja de Muertos Island, Cayo Morillito, and Cayo Berbería (Figure 1). However, in this study, only Caja de Muertos Island and Cayo Morillito were considered, because these areas have the largest historical aerial photographic record, which was used for analyzing long-term changes in seagrass cover (León-Pérez *et al.*, unpublished data). The boundary of the study area was delimited by the lesser of two factors: a maximum depth of 12 m, according to National Oceanic and Atmospheric Administration (NOAA) Nautical Chart 25677 (NOAA, 2018a), or 1 km of maximum distance from the coast. These factors were determined based on three criteria: the capability of identifying seagrass in the historical photographs, the *Thalassia testudinum* colonization limit (Short *et al.*, 2010), and field logistics.

Caja de Muertos Island is located at latitude 17°53′35.5″ N and longitude 66°31′14.9″ W in the Caribbean Sea and is approximately 2.75 km long by 0.85 km wide at its widest point. The west side is protected from the prevailing wind and wave energy direction from the E and SE. In general, differences in bathymetry and geophysical characteristics create a heterogeneous seascape composed of coral reefs, seagrass, macroalgae, and hard and sandy bottoms (García-Sais and Sabater, 2001).

The climatology of Puerto Rico is characterized by a dry season from December through April and a rainy season from May through November (Glynn, 1973). The S coast of Puerto Rico receives significantly less annual precipitation than the N coast (Miller and Lugo, 2009). Since Caja de Muertos Island is located 8.3 km off the S coast of Puerto Rico, the influence of land-based sources of pollution is minimal, and clear-water conditions predominate year-round.

These conditions make Caja de Muertos Island a popular recreational area for visitors that access the island by ferry or private boats. The Puerto Rico Department of Natural and Environmental Resources (DNER) manages the island for recreation and conservation purposes. For example, the DNER maintains a number of mooring buoys to prevent anchor damage to seagrass and other habitats. Public access to Morillito Key and the beach on the S side of Caja de Muertos is not allowed to protect seabird and sea turtle nesting areas from disturbance. In addition, the DNER designated a no-take zone in 2010 in the NE part of the island, an area that can only be used with DNER permits for snorkeling or research purposes. Private boat visitors usually tie up to a mooring buoy or anchor in the W and NW areas of the island.

Image Data Acquisition and Preprocessing

A 16 October 2014 multispectral image from the WorldView-2 (WV-2) sensor was acquired for Caja de Muertos Island (Image ID: 103001003868A000). This archived image was selected because of the absence of clouds and sunglint; it has an off-nadir viewing angle of 26.4° and a sun elevation of 60.3°. The image consisted of one panchromatic band and eight multispectral bands of 0.5 m and 2 m spatial resolution, respectively.

Image preprocessing steps were performed by an external service provider (Earth Observation & Environmental Services | EOMAP), who used the Modular Inversion and Processing System (MIP) proprietary software package (Heege, 2000; Heege *et al.*, 2004; Kiselev, Bulgarelli, and Heege, 2015). These modules were applied to correct the satellite sensor noise, atmospheric effects, influence of adjacent land reflectance, turbidity, tidal influence, and water-column attenuation. The retrieval of the atmospheric optical thickness and water-column constituents was conducted by minimizing the mean square difference between the modeled top-of-atmosphere radiances and the radiances measured for all sensor channels (Heege *et al.*, 2009). The WATCOR module was used for water depth and seafloor determinations (Heege *et al.*, 2004; Pinnel, 2007). The equations published by Albert and Mobley (2003) were the basis for transforming the subsurface reflectance to seafloor albedo. Additional details on the processing steps and algorithms used can be obtained from Albert and Mobley (2003), Heege (2000), Heege *et al.* (2004, 2009), Kiselev, Bulgarelli, and Heege (2015), Pinnel (2007), and Siermann *et al.* (2014). The final products delivered by EOMAP included the bathymetry and seafloor reflectance products for the WV-2 image of Caja de Muertos Island.

Field Data Acquisition and Analysis

Benthic habitat types were verified using 127 sampling sites that were visited during March and June of 2015. Because of the absence of major atmospheric episodic events and since seagrass seasonal variations in the tropics are less pronounced (Erftemeijer and Herman, 1994; Lanyon and Marsh, 1995), no significant temporal changes were expected in the benthic
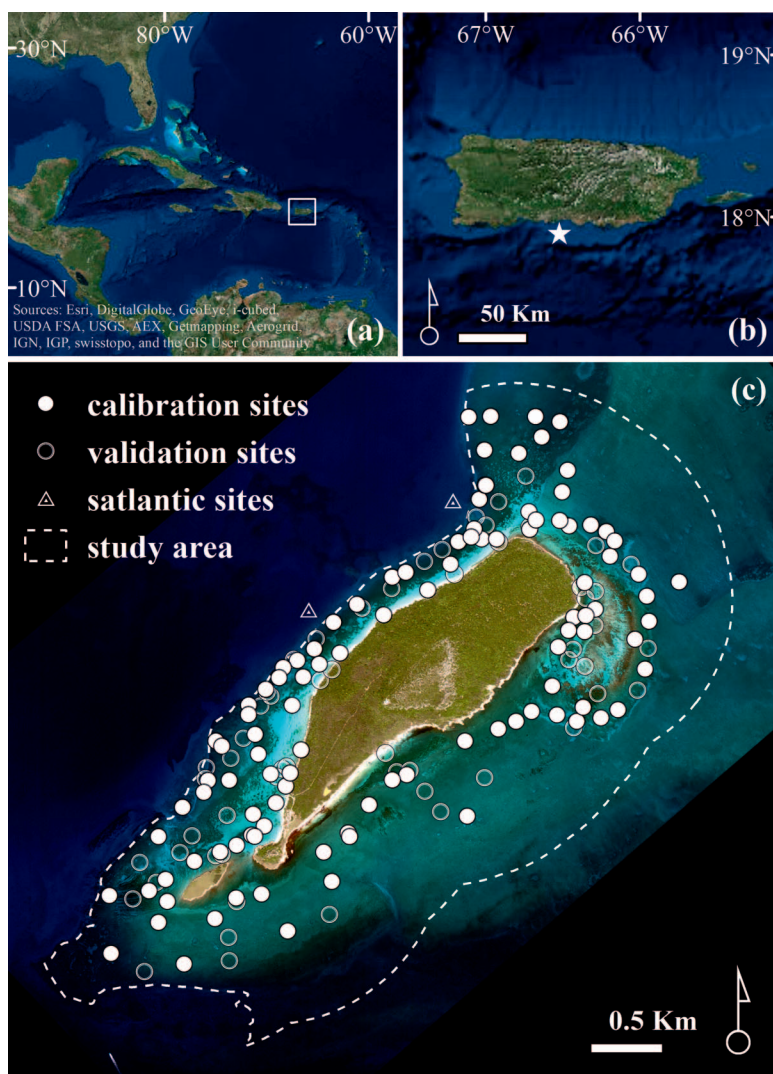
Figure 1. (a) Location of Puerto Rico (white rectangle) in the Caribbean Sea. (b) The study area around Caja de Muertos Island, located south of Puerto Rico (white star). (c) The WV-2 image of Caja de Muertos Island, showing the study area boundary, and the calibration and validation sites used for the creation of the seagrass benthic and bathymetry maps.

cover between the image acquisition date and field sampling period for the current mapping effort. Ninety-nine sites were selected randomly beforehand and visited during March 2015. Due to a GPS unit malfunction during the last sampling effort in June 2015, the exact position of the 27 sites that where selected beforehand could not be visited. Thus, a zigzag navigational pattern was used to sample those 27 sites within the boundary of the study area. A Trimble® Juno 3D GPS was used for navigating to the sampling locations and for the captain to maneuver the boat and maintain its position. An on-board submersible high-definition video camera (Delta Vision HD camera) was used for recording a 10 second video of the benthos at each site. While the video was being recorded, 10 seconds of geographic coordinates were recorded and averaged by the Juno GPS (1–4 m accuracy), except during the June sampling, when GPS coordinates were recorded using a

Garmin GPS Map 72 (3–5 m accuracy). Once in the laboratory, snapshots of the videos were taken at approximately the 5 second mark of the recording, and these represented the benthos of that site. The shallow back reef at the NE end of the island had to be surveyed using snorkeling gear and a Nikon Coolpix AW110 digital camera. Using the boat depth sounder, depth was recorded in all sampling sites.

Vertical hyperspectral profiles of downwelling irradiance were measured using a Satlantic HyperPro spectroradiometer and were used to calculate spectral attenuation coefficients (K_d) at the midpoints of the WV-2 bands, and $K_{d\ PAR}$ (photosynthetic available radiation [PAR]) at two sites on the N and W sides of the island (Figure 1). Both measurements were averaged for the analysis. The optical depth of the midpoints of the WV-2 bands was calculated as $1/K_d$ and was used to determine the WV-2 bands that were suitable for the image analysis. In

addition, $K_{d\ PAR}$ was calculated and used to determine the depth of the euphotic zone (1% of surface light) as $4.6/K_{d\ PAR}$ and the midpoint of the euphotic zone (10% of surface light) as $2.3/K_{d\ PAR}$ (Kirk, 2011).

All sampling sites were assigned one of the following benthic habitat classification categories (first classification level): seagrass, colonized hard bottom, sand, and macroalgae. A second classification level was defined for the seagrass and colonized hard bottom categories. The seagrass subcategories used were similar to the categories used by Lyons, Phinn, and Roelfsema (2012), where the seagrass projected horizontal cover was subcategorized into: sparse (1% to 40% cover), moderate (40% to 70%), and dense (70% to 100%). The same percentage classifications were used for the colonized hard bottom subcategories, which consisted of consolidated grounds either covered by turf algae, sponges, and corals or a combination of them. Sand and macroalgae were also identified in the field data and therefore included in the classification scheme. The macroalgae category was mainly composed of sand colonized by the green algae *Cymopolia barbata* and/or different species of green, red, or brown algae. Percent cover of the seagrass and colonized hard bottom subcategories was determined by using a uniform grid of 36 points for each snapshot in the benthic cover assessment program Coral Point Count Excel V4.1 (Kohler and Gill, 2006).

The sampling sites were designated either for calibration or validation of the benthic habitat map (Figure 1). Following Roelfsema *et al*. (2014), approximately two-thirds of each benthic habitat category were designated for calibration, and one-third was used for validation. Due to the limited number of sites, the validation sites for the seagrass category did not include sites representing the sparse seagrass subcategory. Additional sites were included based on the researchers' knowledge of the study area to increase the number of sites for categories with low numbers. The new sites were randomly assigned either to calibration or validation as needed. In total, 106 calibration sites were used to train the image data and conduct a supervised classification, and 58 validation sites were used to assess the accuracy of the classification output.

Classification Approach

The seafloor reflectance image provided by EOMAP was processed using a multiresolution segmentation algorithm, an OBIA, in eCognition Essentials 1.2 (Trimble). During this step, three corrected WV-2 bands and the bathymetry data were used (see "Results" section for details). The process of optimizing the parameters for the segmentation process was conducted as an iterative trial-and-error process (Lathrop, Montesano, and Haag, 2006). The selected scale, color/shape, and smoothness/compactness weights were 20, 0.05, and 0.8, respectively. The minimum size of the objects created during the segmentation was 4 m^2, which corresponds with the minimum mapping unit. Afterward, series of threshold classifications were used to differentiate between masked areas (land and areas outside the delimited study area) and water, and between sand and the other benthic categories. Objects that were not classified in the threshold classification were subject to a supervised classification (Decision Tree algorithm) using the training samples derived from the calibration field data. Contextual editing, described by Mumby *et al*. (1998) as a tool that may significantly increase the classification accuracy for mapping coral reefs with multispectral data, was used to visually reclassify objects (individual polygons) that were not accurately classified, based on the field data and the researchers' knowledge of the area.

Accuracy Assessment

The validation sites were used to evaluate the classification output. An error matrix was created to evaluate the classification accuracy of each benthic habitat category and to calculate the producer's and user's accuracy (Schowengerdt, 1983). The producer's accuracy, or omission error, indicates the probability of a reference pixel being correctly classified in the map, while the user's accuracy, or commission error, indicates the probability that a pixel classified on the map indeed represents that category on the ground (Congalton, 1991).

Additionally, a reliability map was created for the entire study area to quantify the reliability level of each classified object. This map was developed in order to compensate for limitations in the number of validation sites for some benthic categories and to provide an additional tool with which to evaluate the accuracy of the benthic habitat map. Each polygon was assigned a reliability level based on two criteria (modified from Roelfsema *et al*., 2013): a ratio of sampling sites per object area, and the researchers' expert knowledge. A ratio of sampling sites per object area was calculated and a weighted value between 1 and 3 was assigned for each object, where the value of 3 indicated objects that were better represented by the sampling sites. This procedure was done to account for size differences between the areas of each object. The researchers' expert knowledge criterion was based in the authors' confidence (based on their experience of visually identifying benthic habitat in WV-2 imagery and their knowledge of the study area) to assign a benthic category to a particular object while conducting the contextual editing step. This expert criterion was also assigned a weighted value between 1 and 3, where 3 was the most confident value. The following equation was used to calculate reliability level: ratio of sampling sites per object area + researchers' expert knowledge = estimated reliability level. A reliability level between 1 and 2 is considered low, 3 is medium, and 4 to 6 is high.

A regression analysis comparing the field-collected water depth *vs*. the bathymetric map-derived data was conducted to assess the accuracy of the bathymetry map.

RESULTS

The results are presented in four subsections: benthic field data, light penetration, seagrass benthic map and accuracy assessment, and bathymetry map and its validation.

Benthic Field Data

From the 127 sites visited, 43.97% were composed of colonized hard bottom, and 43.26% were composed of seagrass (Figure 2). Among the visited sites with seagrass, more than half (62.30%) were classified as dense seagrass, followed by moderate seagrass (26.23%) and sparse seagrass (11.48%). Sand and macroalgae represented the minority of the visited sites, representing 7.80% and 4.96%, respectively.
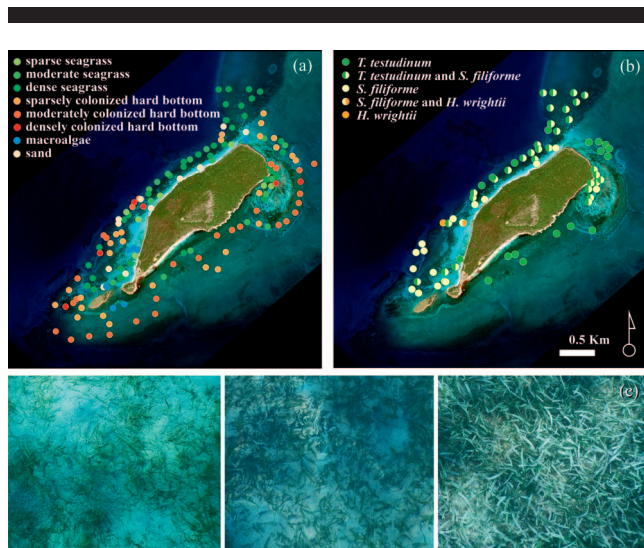
Figure 2. (a) Benthic habitat categories of each calibration and validation site in which seagrass was the second most common category, composed mainly of dense seagrass. (b) All sites where seagrass was identified, almost half of which were composed of a combination of *T. testudinum* and *S. filiforme*. (c) Examples of underwater snapshots of the three seagrass subcategories from sparse to dense (left to right).
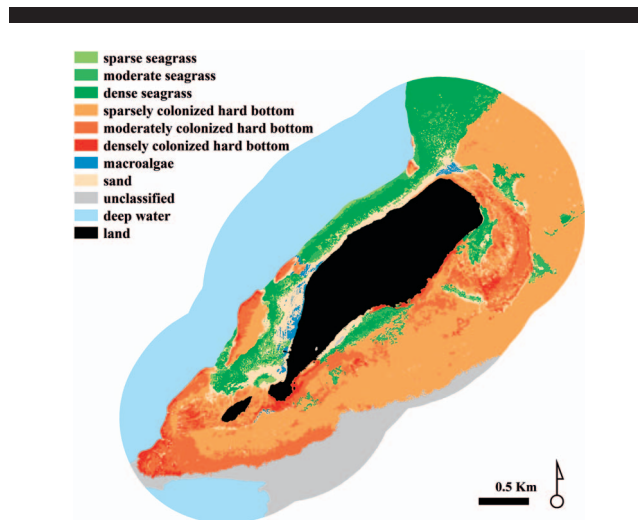

Figure 3. Benthic habitat categories mapped within the CMINR study area derived from WV-2 image and field data. Seagrass habitats represented the second most abundant benthic habitat and were mainly distributed N and W of Caja de Muertos Island.

Three seagrass species were identified in the study area: *T. testudinum*, *Syringodium filiforme*, and *Halodule wrightii*. Sites with coexisting *T. testudinum* and *S. filiforme* represented almost half (47.83%) of the sites where seagrass was present, followed by *T. testudinum* (26.09%) and *S. filiforme* (23.19%) individually. *Halodule wrightii* was only identified in two sites. *Halophila stipulacea*, an invasive seagrass species previously documented in Puerto Rico (Ruiz and Ballantine, 2004), was not present in the sites visited during this study.

Light Penetration

Measurements taken with the Satlantic Hyper Pro spectroradiometer were averaged and used to calculate the optical depths at WV-2 wavelengths. The optical depths calculated revealed that the coastal (B1), blue (B2), and green (B3) bands had the deepest optical depths of the WV-2 visible bands, covering the depth range of the study area (0–12 m) (Table 1). Therefore, these bands were used for the creation of the seagrass benthic map. The yellow (B4) and red (B5) bands were excluded from the analysis since they were rapidly absorbed in the water column (Table 1).

The depth of the euphotic zone, where 1% of the photosynthetic available radiation reaches, was 43.38 m, and the

midpoint of the euphotic zone (10% of surface irradiance) was 21.69 m.

Seagrass Benthic Map and Accuracy Assessment

Almost eight square kilometers (7.56 km^2) of benthic habitat were mapped around Caja de Muertos Island (Figure 3). Sparsely colonized hard bottom covered most of the study area, representing 43.57% of the total area (Table 2). Seagrass habitats (dense, moderate, and sparse) accounted for the second most abundant benthic habitat, covering 1.49 km^2 (19.67%) and was mainly present in the N and W sides of the island. The dense seagrass subcategory represented 55.79% of the total seagrass area, followed by the moderate and sparse seagrass subcategories. The last two were mainly found in the transition zones between seagrass beds and other habitats, and within "blow-outs," which are small rounded depressions cause by strong wave action.

Due to unsuitable weather conditions, field visits to the far south of the study area were not possible. Consequently, 11.80% of the study area could not be accurately mapped and was classifed as "unclassifed." Areas previously classified as deeper than 12 m were omitted from the analysis and classified as "deep water."

The combination of the mapping techniques resulted in an overall accuracy of 96.59% and a seagrass overall accuracy of 100% for the CMINR study site. An error matrix with the user and producer accuracy analysis is shown in Table 3. The seagrass, colonized hard bottom, and sand categories had a producer accuracy of 100%. The moderate and dense seagrass subcategories had a producer accuracy above 80%. The limited field sites that represented the sparse seagrass category were used for calibrating the benthic map, and so no validation sites were left for the accuracy assessment of this category. When analyzing the user accuracy, the seagrass category had a 100% probability of being represented as such in the map.

Table 1. *WV-2 bands optical depths calculated using the field-measured K_d values.*

Band Number	Band Center (nm)	K_d (m^{-1})	Optical Depth (m)
Coastal	425	0.0728	13.7
Blue	480	0.0555	18.0
Green	545	0.0811	12.3
Yellow	605	0.2859	3.0
Red	660	0.4070	2.4

Table 2. *Area covered by each benthic habitat category within the study area.*

Benthic Habitat Categories and Subcategories	Area (km^2)	Percent (%)	Percent of Seagrass (%)
Seagrass	1.486	19.67	100
Sparse seagrass (10%–40%)	0.2561	3.39	17.23
Moderate seagrass (40%–70%)	0.4009	5.31	26.98
Dense seagrass (70%–100%)	0.8290	10.97	55.79
Colonized hard bottom	4.5998	60.87	100
Sparsely colonized hard bottom (10%–40%)	3.2924	43.57	n/a
Moderately colonized hard bottom (40%–70%)	1.0594	14.02	n/a
Densely colonized hard bottom (70%–100%)	0.2480	3.28	n/a
Macroalgae	0.0616	0.82	n/a
Sand	0.5173	6.85	n/a
Unclassified	0.8914	11.80	n/a
Total	7.5561	100	100

Given these limitations, a reliability analysis was conducted in order to further assess map accuracy. Figure 4 shows the level of reliability based in a ratio of sampling sites per object area and researchers' expert knowledge for each object classified in the map. Since the optical depths of the coastal, blue, and green bands used for the OBIA were deeper than the 12 m study area boundary, a depth criterion was not included in the reliability map. The dominant reliability level was medium, for 3.60 km^2, representing 53.93% of the total area, followed by high (23.45%) and low (22.61%) (Table 4). However, when looking only at the seagrass category, 52.97% of seagrass had a reliability level of high, followed by medium (31.78%) and low (15.25%) (Table 4).

Bathymetry Map and its Validation

The WV-2 bathymetry data for the study area ranged from 0.2 to −13.5 m (Figure 5). The W and SW sides of the island are characterized by a steep drop off at approximately 250 m from the shore at its nearest point. On the other hand, the E and NE sides of the island have a smoother slope and the presence of shallow reef lagoon.

Seagrass was present in all depths of the study area. However, almost half (48.17%) was distributed between 6 to 9 m and mainly fell in the dense seagrass subcategory (Figure 6). The lesser amount of seagrass was distributed within very shallow (0 to 1 m; 7.12%) and deeper parts (10 to 13 m; 8.00%) of

the study area. The maximum values for the moderate and sparse categories were observed within 2 to 3 m depths.

The WV-2 bathymetry data were plotted against the field-collected depth data to validate how well it estimated depth (Figure 7). The bathymetry data successfully estimated depth values with an $r^2 = 0.94$; however, a slight underestimation was observed in shallow zones, and the opposite was observed in deeper zones.

DISCUSSION

A 2014 high-resolution seagrass benthic map was successfully created for the CMINR study area. This map shows that seagrass is distributed throughout the study area, except the S, and within all depths. In this respect, and in concurrence with the findings by Otero *et al.* (2014), the light attenuation data suggest that seagrass colonization in the study area is not limited by PAR availability. The calculation of the midpoint of the euphotic zone, a relevant optical depth for primary production and seagrass colonization (Duarte, 1991; Kirk, 2011), suggests that seagrass could be present up to a depth of ~22 m in the CMINR.

The dense seagrass subcategory represented the majority of the total seagrass area mapped and was mainly present in the N and W parts of the study area. Seagrass beds in these areas were mostly composed of *T. testudinum* mixed with *S. filiforme*. Although *T. testudinum* has been known to be a climax species

Table 3. *Accuracy assessment for the benthic habitat categories derived from the WV-2 image of CMINR. Bold diagonal elements represent sites that were correctly classified. Se = seagrass; SS = sparse seagrass; MS = moderate seagrass; DS = dense seagrass; CH = colonized hard bottom; SCH = sparsely colonized hard bottom; MCH = moderately colonized hard bottom; DCH = densely colonized hard bottom; Ma = macroalgae; Sa = sand; T = total; PA = producer accuracy; UA = user accuracy.*

Validation Data	Calibration Data											
	Se	SS	MS	DS	CH	SCH	MCH	DCH	Ma	Sa	T	PA (%)
Se	**20**	0	0	0	0	0	0	0	0	0	20	100
SS	0	**0**	0	0	0	0	0	0	0	0	0	0
MS	0	1	**4**	0	0	0	0	0	0	0	5	80.00
DS	0	0	2	**13**	0	0	0	0	0	0	15	86.67
CH	0	0	0	0	**21**	0	0	0	0	0	21	100
SCH	0	0	0	0	0	**8**	1	0	0	0	9	88.89
MCH	0	0	0	0	0	2	**7**	0	0	0	9	77.78
DCH	0	0	0	0	0	0	2	**1**	0	0	3	33.33
Ma	0	0	0	0	1	1	0	0	**5**	1	7	71.43
Sa	0	0	0	0	0	0	0	0	0	**10**	10	100
T	20	1	6	13	22	11	10	1	5	11	80	
UA (%)	100	0	66.67	100	95.45	72.73	70.00	100	100	90.91		

Overall accuracy = 96.59%
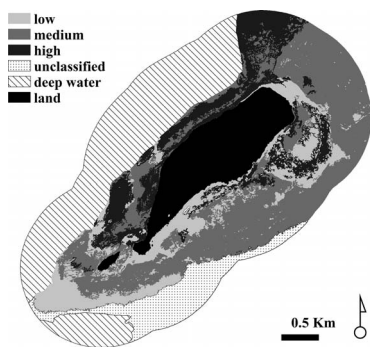*Seagrass accuracy = 100%*

Figure 4. Reliability of benthic habitats categories mapped in the CMINR study area shows that more than half of the seagrass areas were mapped with a high reliability level.
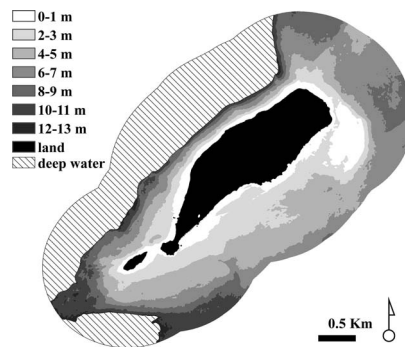

Figure 5. WV-2 bathymetry map for the CMINR study area shows a steep drop off located W and SW of Caja de Muertos Island and a smoother slope E and NE of the island.

(Creed, Phillips, and van Tussenbroek, 2003), the coexistence of more seagrass species in a Caribbean *T. testudinum* community may be caused by niche partitioning when the community comes closer to its climax state (Williams, 1990). This may be the case for dense seagrass communities in the W part of the study area and some areas in the N within the study area and could be a result of a combination of favorable environmental conditions, since, for example, these areas, located mainly within 6 to 9 m depth, are less susceptible to frequent wave action in comparison with other areas where blowouts dominate the seascape. The coexistence of *T. testudinum* and *S. filiforme* was also documented in the NE reef lagoon. Although this area is shallower (<3.4 m), it is sheltered from the incoming wave energy, and so it may be less subject to burial and sediment removal that could alter its stability. Dense seagrass composed mainly of monospecific stands of *T. testudinum* was also found, although to a lesser extent, in other areas unprotected from the incoming wave energy around Caja de Muertos Island. This species can form dense rhizomes (Creed, Phillips, and van Tussenbroek, 2003), and experimental manipulations conducted by Cruz-Palacios and van Tussenbroek (2005) showed it to be almost undamaged by burial and sediment removal.

The high-spatial-resolution map revealed areas where seagrass has suffered the impacts of strong wave action. This assumption is supported by the presence of blowouts in the N region of the study area exposed to the wave direction from the E, which are mainly present in depths between 4 and 7 m.

Table 4. *Total benthic habitat and seagrass area covered by each reliability level in the study area.*

Reliability Level	Total (km^2)	Percent (%)
Total benthic habitat area		
Low	1.5070	22.61
Medium	3.5946	53.93
High	1.5631	23.45
Total	6.6647	100
Total seagrass area		
Low	0.2266	15.25
Medium	0.4722	31.78
High	0.7872	52.97
Total	1.4860	100

Other researchers (Gonzalez-Liboy, 1979; Rodriguez, Webb, and Bush, 1994) have reported significant losses of seagrass in other areas in Puerto Rico due to intense periods of wave action that have created blowouts. Blowouts can be identified in Figure 8 as areas within dense seagrass meadows interrupted by small rounded areas with moderate and/or sparse seagrass and/or sand. Field data revealed that areas of the sparse seagrass subcategory were mainly composed of *S. filiforme* and *H. wrightii*, which are known pioneer species (Williams, 1990) that can propagate and colonize areas faster than *T. testudinum* (Tomlinson, 1974). The delicate rhizomes and root system of *S. filiforme* make it more susceptible to detachment than *T. testudinum* during disturbance events (Cruz-Palacios and van Tussenbroek, 2005). Thus, areas dominated by fast-growing seagrass species, such as *S. filiforme*, may be an indication of areas more susceptible to periodical disturbances. Besides blowouts, maximum values for moderate and sparse subcate-
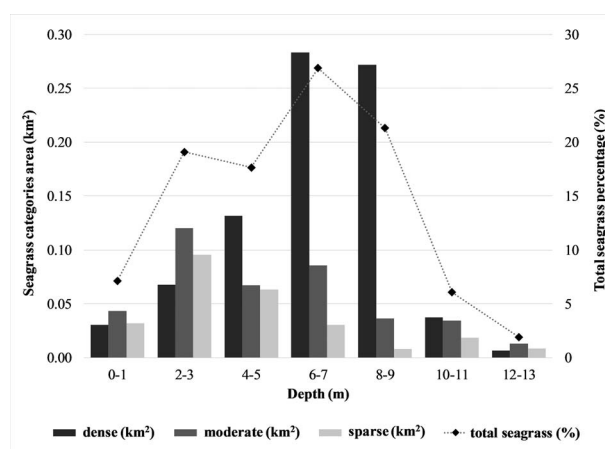

Figure 6. Seagrass depth distribution in the CMINR study area shows the area occupied by each seagrass subcategory and the total seagrass percentage along the depth gradient. Seagrass was mapped in all depths of the CMINR study area, but almost half was distributed between 6 to 9 m depth.
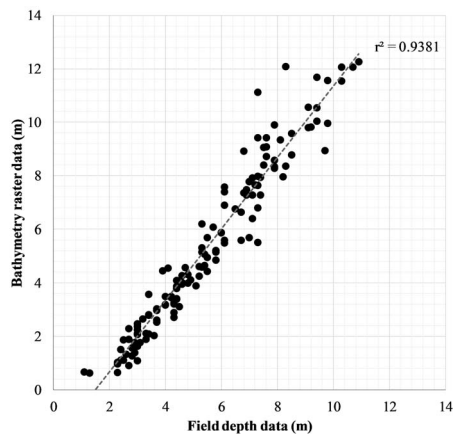
Figure 7. The regression analysis shows a linear relationship between the WV-2–derived bathymetry raster data and field depth data.
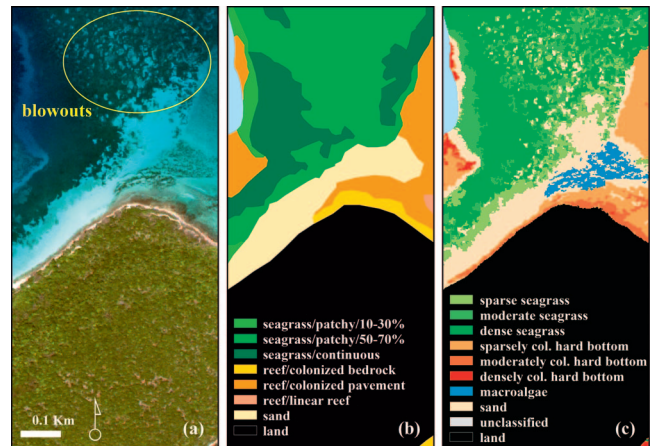

Figure 8. A close-up of the N side of the study area for the (a) raw 2014 WV-2 image, (b) NOAA benthic habitat map (Kendall *et al.*, 2001), and (c) WV-2 seagrass benthic map. This comparison shows how the WV-2 seagrass benthic map is more suitable to detect small features such as blowouts.

gories were observed between 2 and 3 m depth, which are areas more susceptible to wave action.

The seagrass area mapped represented 22.13% more than the previous benthic map available for the study area (Kendall *et al.*, 2001). Although this increase could represent a real change in the seagrass community that occurred during the 15 years that passed between these two mapping efforts, a direct comparison cannot be made due to the differences in the data and methods used. Kendall *et al.* (2001) used a natural color aerial photograph taken in 1999 and a visual classification technique, while in the present study, a WV-2 image was used together with a combination of an OBIA, supervised classification, and contextual editing. These difference in the remotely collected data and in the classification approach could contribute to the differences observed. In addition, in this study, the minimum mapping unit was considerably reduced from 4047 m^2 (Kendall *et al.*, 2001) to 4 m^2, allowing for the discrimination between different seagrass density categories and areas of sand between the seagrass beds that were previously mapped as a single category by Kendall *et al.* (2001) (Figure 8).

When compared with other benthic maps in Puerto Rico, the accuracy obtained (96.59% overall accuracy and 100% seagrass overall accuracy) is above published accuracy values for benthic habitat mapping. Kendall *et al.* (2001) validated the Puerto Rico benthic habitat map in La Parguera Nature Reserve and obtained an overall accuracy of 93.60%. Although these authors suggested that other areas with similar conditions to La Parguera would also be mapped with comparable accuracies, this could potentially lead to misinterpretation of certain benthic habitat categories outside of La Parguera. On the other hand, Hernández-López (2015) obtained a lower overall accuracy of 64.81% and a 75.00% seagrass accuracy using an ISODATA classification of a WV-2 image also from La Parguera.

The seagrass, colonized hard bottom, and sand categories were accurately mapped, having zero omission error (Table 3). Seagrass subcategories were also accurately mapped, with the

exception of the sparse seagrass subcategory that was not assessed. The small error associated with the producer accuracy of the dense and moderate seagrass subcategories was attributed to confusion with other seagrass subcategories, which can be expected from mapping continuous habitat into discrete categories, since areas close to the category boundary have a higher probability of being misclassified (Lyons, Phinn, and Roelfsema, 2011). Similar to the sparse seagrass subcategory, a limitation in the number of validation sites for the densely colonized hard bottom subcategory prevented a suitable assessment of its accuracy.

A reliability analysis was conducted to compensate for the limitations in the number of validation sites for some benthic categories and to provide an additional tool with which to evaluate the accuracy of the seagrass benthic map. More than half of the mapped seagrass had a high reliability level (52.97%) and was mainly composed of the dense seagrass subcategory (87.19%), the most abundant seagrass subcategory mapped. Areas with low reliability were mainly located in the S, E, and NE parts of the study area, where less expert knowledge and fewer sampling sites were available. As mentioned by Roelfsema *et al.* (2009), the reliability map may not be an ideal approach with which to assess map accuracy; however, it provides the users a tool for deciding the areas of the map that are more reliable.

In terms of the water depth data, the WV-2 bathymetry map retrieved accurate values of depth; however, a small offset (~1 m) was observed in the regression analysis (Figure 7), which can be associated with some sources of error. A source of error present, but considered minimal, is the fact that the WV-2 image was corrected for tidal influence, but the field values were not. This source of error is considered to be insignificant, since changes in the tide range in this region are mainly less than 0.3 m (NOAA, 2018b). However, sources of error associated with horizontal displacement could have contributed to the observed offset. These are the displacements of the

boat due to currents, waves, and wind, the accuracy error of the GPS, and the distance between the locations where the geographic coordinates and depth measurements were taken in the boat. Nevertheless, most of the seagrass mapped was within 6 to 9 m depth, where the bathymetry data were reliable. This bathymetry map accuracy compares with that of Hernandez and Armstrong (2016), who obtained a similar accuracy ($r^2 = 0.90$) in a bathymetry map generated for La Parguera, Puerto Rico, with the same multispectral sensor.

Overall, the methods used in this study proved to be effective for mapping seagrass within a highly complex benthic environment. The use of a WV-2 image together with the combination of OBIA, supervised classification, and contextual editing enhanced the mapping process, reducing human intervention and increasing the ability for delineating benthic features in the image. Contrary to the manual delineation of benthic features used in previous mapping efforts (Kendall *et al.*, 2001), the use of OBIA automatized the process and reduced the number of personnel hours. In this study, human intervention was constrained and used during the contextual editing step to improve areas where the supervised classification performed poorly. Additionally, the use of the Satlantic Hyper Pro optical data helped in discriminating the WV-2 bands that were suitable for the image analysis, but, more importantly, it was used for determining the seagrass colonization limit in the study area. Finally, the development of a reliability map provided managers and users with another metric for evaluating the map accuracy.

A more recent NOAA mapping effort in Puerto Rico used a similar approach to this study, using atmospheric- and water column–corrected WV-2 imagery, a supervised classification, and manual edits (Kågesten *et al.*, 2015). However, that effort did not include CMINR. Therefore, the present mapping effort represents the most recent and reliable benthic seagrass habitat map for CMINR.

The present study provides relevant information for the management of the CMINR. The W and NW sides of Caja de Muertos Island, which contain most of the seagrass cover from the study area, are also the most frequented areas by visitors. Excluding the shallow seagrass bed within the reef lagoon in the NE, which requires a permit to enter by boat, the seagrass beds in the frequently visited areas are deep enough to prevent propeller scarring, which was not observed during the field work. Furthermore, in order to minimize anchor damage to benthic habitats in the W and NE sides of the island, the DNER has installed and maintains mooring buoys. DNER could use this study to identify areas to install additional mooring buoys if necessary. On the other hand, managers can also use the seagrass benthic map for assessing the impacts of extreme weather events occurring after 2014, such as hurricanes, on the abundance and distribution of seagrass. Changes in the bathymetry of the mapped area after such events could be assessed, along with their implications for seagrass dynamics. Subsequent seagrass restoration efforts could be guided using these data. In the case of *Halophila stipulacea* colonizing in the reserve, these data could be used to assess changes in the benthic landscape caused by its colonization. Finally, the information presented here could serve the DNER as a reference to guide future marine spatial planning of the reserve.

CONCLUSIONS

This study produced a satellite-derived, field-validated map to serve as baseline information on the distribution of benthic communities in CMINR with particular focus on seagrass habitats. This work improved upon previous mapping efforts conducted in the reserve through the development of more recent, high-resolution, and accurate seagrass benthic habitat and bathymetry maps. Therefore, this map represents the first high-spatial-resolution benthic habitat map for CMINR. The methods used in this study proved to be effective for mapping seagrass habitats in optically clear waters and could be replicated in areas with similar environmental conditions.

In general, seagrasses in CMINR were found in diverse scenarios of wave energy exposure, depth, geographic location, and species composition. In these clear, oligotrophic waters, photosynthetically available light is not a limiting factor for seagrass colonization within the study area. Periods of strong wave energy may be important in regulating seagrass distribution, as it was evident north of Caja de Muertos Island where blowouts were identified. Results suggest that seagrass beds in the study area are more subject to the influence of storm surges than impacts of boating activities or other anthropogenic threats.

The results of this study can be used by agencies tasked with conserving and managing marine ecosystems. Some of the potential uses of this baseline map include: assessing future impacts of episodic atmospheric events on seagrass communities; evaluating potential anthropogenic impacts on seagrass communities, such as boat propeller scars in shallow areas; monitoring changes in seagrass cover associated with the colonization of *H. stipulacea* in the reserve; selection of new locations for installing mooring buoys; and for other management and spatial planning activities within the reserve.

LITERATURE CITED

Albert, A. and Mobley, C.D., 2003. An analytical model for subsurface irradiance and remote sensing reflectance in deep and shallow case-2 waters. *Optics Express*, 11(22), 2873–2890.

Armstrong, R.A., 1981. Changes in a Puerto Rican coral reef from 1936–1979 using aerial photoanalysis. *Proceedings of the 4th International Coral Reef Symposium* (Manila, Philippines), Volume 1, pp. 309–315.

Armstrong, R.A., 1993. Remote sensing of submerged vegetation canopies for biomass estimation. *International Journal of Remote Sensing*, 14(3), 621–627.

Congalton, R.G., 1991. A review of assessing the accuracy of classifications of remotely sensed data. *Remote Sensing of the Environment*, 37(1), 35–46.

Costanza, R.; dArge, R.; de Groot, R.; Farber, S.; Grasso, M.; Hannon, B.; Limburg, K.; Naeem, S.; Oneill, R.V.; Paruelo, J.; Raskin, R.G.; Sutton, P., and van den Belt, M., 1997. The value of the world's ecosystem services and natural capital. *Nature*, 387(6630), 253–260.

Creed, J.C.; Phillips, R.C., and van Tussenbroek, B.I., 2003. Seagrasses of the Caribbean. *In:* Green, E.P., and Short, F.T. (eds.), *World Atlas of Seagrasses*. Berkeley, California: University of California Press, 300p.

Cruz-Palacios, V. and van Tussenbroek, B.I., 2005. Simulation of hurricane-like disturbances on a Caribbean seagrass bed. *Journal of Experimental Marine Biology and Ecology*, 324(1), 44–60.

Duarte, C.M., 1991. Seagrass depth limits. *Aquatic Botany*, 40(4), 363–377.

Duarte, C.M., 2002. The future of seagrass meadows. *Environmental Conservation*, 29, 192–206.

Erftemeijer, P.L.A. and Herman, P.M.J., 1994. Seasonal changes in environmental variables, biomass, production and nutrient contents in two contrasting tropical intertidal seagrass beds in South Sulawesi, Indonesia. *Oecologia*, 99(1–2), 45–59.

García-Sais, J.R. and Sabater, J., 2001. *Coral Reef Communities from Natural Reserves in Puerto Rico: A Baseline Quantitative Assessment for Prospective Monitoring Programs*. San Juan, Puerto Rico: DNER and NOAA coral Reef Conservation Program. *Final Report submitted DNER U.S. Coral Reef National Monitoring Program– NOAA*, 134p.

Glynn, P.W., 1973. Ecology of a Caribbean coral reef: The Porites reef flat biotope: Part I, Meteorology and hydrography. *Marine Geology*, 20(4), 297–318.

Gonzalez-Liboy, J., 1979. *An Examination of the Present Condition of Seagrass Meadows in La Parguera, Puerto Rico*. San Juan, Puerto Rico: DNER and U.S. Fish and Wildlife Service, *Final Report to the Department of Natural Resources and U.S. Fish and Wildlife Service*, 100p.

Heege, T., 2000. Flugzeuggestützte Fernerkundung von Wasserinhaltsstoffen am Bodensee. Berlin, Germany: Freie Universität Berlin, Ph.D. dissertation, 134p.

Heege, T.; Bogner, A.; Pinnel, N.; Bostater, C.R., and Santoleri, R., 2004. Mapping of submerged aquatic vegetation with a physically based process chain. *Remote Sensing of the Ocean and Sea Ice*, 5233, 43–50.

Heege, T.; Kiselev, V.; Odermatt, D.; Heblinski, J.; Schmieder, K.; Khac, T.V., and Long, T.T., 2009. Retrieval of water constituents from multiple Earth observation sensors in lakes, rivers and coastal zones. *Proceedings International Geoscience and Remote Sensing Symposium* (Cape Town, South Africa), pp. 3–6.

Hernandez, W.J. and Armstrong, R.A., 2016. Deriving bathymetry from multispectral remote sensing data. *Journal of Marine Science and Engineering*, 4(1), 8.

Hernández-Cruz, L.R.; Purkis, S., and Riegl, B., 2006. Documenting decadal spatial changes in seagrass and *Acropora palmata* cover by aerial photography analysis in Vieques, Puerto Rico: 1937–2000. *Bulletin of Marine Science*, 79(2), 401–414.

Hernández-López, W.L., 2015. Benthic Habitat Mapping and Bio-Optical Characterization of La Parguera Marine Reserve using Passive and Active Remote Sensing Data. Lajas, Puerto Rico: University of Puerto Rico, Mayagüez Campus, Ph.D. dissertation, 164p.

Hoang, T.; Garcia, R.; O'Leary, M., and Fotedar, R., 2016. Identification and mapping of marine submerged aquatic vegetation in shallow coastal waters with WorldView-2 satellite data. *In:* Vila-Concejo, A.; Bruce, E.; Kennedy, D.M., and McCarroll, R.J. (eds.), *Proceedings of the 14th International Coastal Symposium (Sydney, Australia)*. *Journal of Coastal Research*, Special Issue No. 75, pp. 1287–1291.

Kågesten, G.; Sautter, W.; Edwards, K.; Costa, B.; Kracker, L., and Battista, T., 2015. *Shallow-Water Benthic Habitats of Northeast Puerto Rico and Culebra Island*. Silver Spring, Maryland: NOAA, *Technical Memorandum NOS NCCOS 200*, 112p.

Kendall, M.S.; Monaco, M.E.; Buja, K.R.; Christensen, J.D.; Kruer, C.R.; Finkbeiner, M., and Warner, R.A., 2001. *Methods Used to Map the Benthic Habitats of Puerto Rico and the U.S. Virgin Islands*. Silver Spring, Maryland: NOAA, 45p.

Kendrick, G.A.; Aylward, M.J.; Hegge, B.J.; Cambridge, M.L.; Hillman, K.; Wyllie, A., and Lord, D., 2002. Changes in seagrass coverage in Cockburn Sound, Western Australia, between 1967 and 1999. *Aquatic Botany*, 73(1), 75–87.

Kirk, J.T.O., 2011. *Light and Photosynthesis in Aquatic Ecosystems*. Cambridge, UK: Cambridge University Press, 662p.

Kiselev, V.; Bulgarelli, B., and Heege, T., 2015. Sensor independent adjacency correction algorithm for coastal and inland water systems. *Remote Sensing of the Environment*, 157, 85–95.

Koedsin, W.; Intararuang, W.; Ritchie, R.J., and Huete, A., 2016. An integrated field and remote sensing method for mapping seagrass species, cover, and biomass in southern Thailand. *Remote Sensing*, 8(4), 292.

Kohler, K.E. and Gill, S.M., 2006. Coral Point Count with Excel extensions (CPCe): A visual basic program for the determination of coral and substrate coverage using random point count methodology. *Computer Geoscience*, 32(9), 1259–1269.

Kovacs, E.; Roelfsema, C.; Lyons, M.; Zhao, S., and Phinn, S., 2018. Seagrass habitat mapping: How do Landsat 8 OLI, Sentinel-2, ZY-3A, and Worldview-3 perform? *Remote Sensing Letters*, 9(7), 686–695.

Lanyon, J.M. and Marsh, H., 1995. Temporal changes in the abundance of some tropical intertidal seagrasses in North Queensland. *Aquatic Botany*, 49(4), 217–237.

Lathrop, G.; Montesano, P., and Haag, S., 2006. A multi-scale segmentation approach to mapping seagrass habitats using airborne digital camera imagery. *Photogrammetric Engineering and Remote Sensing*, 72(6), 665–675.

Lyons, M.; Phinn, S., and Roelfsema, C., 2011. Integrating Quickbird multi-spectral satellite and field data: Mapping bathymetry, seagrass cover, seagrass species and change in Moreton Bay, Australia, in 2004 and 2007. *Remote Sensing*, 3(1), 42–64.

Lyons, M.; Phinn, S., and Roelfsema, C., 2012. Long term land cover and seagrass mapping using Landsat and object-based image analysis from 1972 to 2010 in the coastal environment of South East Queensland, Australia. *ISPRS Journal of Photogrammetry and Remote Sensing*, 71, 4–46.

Maccarrone, V., 2010. Determination of the upper boundary of a Posidonia meadow. *Ecological Information*, 5(4), 267–272.

Miller, G.L. and Lugo, A.E., 2009. *Guide to the Ecological Systems of Puerto Rico*. San Juan, Puerto Rico: U.S. Department of Agriculture, Forest Service, International Institute of Tropical Forestry, *General Technical Report IITFGTR35*, 437p.

Moore, K.; Wilcox, D.; Anderson, B., and Orth, R., 2001. *Analysis of Historical Distribution of Submerged Aquatic Vegetation (SAV) in the York and Rappahannock Rivers as Evidence of Historical Water Quality Conditions*. Gloucester Point, Virginia: Virginia Institute of Marine Science, College of William and Mary *Applied Marine Science and Ocean Engineering Special Report No. 375*, 51p.

Mumby, P.J.; Clark, C.D.; Green, E.P., and Edwards, A.J., 1998. Benefits of water column correction and contextual editing for mapping coral reefs. *International Journal of Remote Sensing*, 19(1), 203–210.

NOAA (National Oceanic and Atmospheric Administration), 2018a. *Nautical Chart 25677*. https://www.charts.noaa.gov/OnLineViewer/25677.shtml

NOAA, 2018b. *Tides and Currents Santa Isabel Station (9756639) 2014*. https://tidesandcurrents.noaa.gov/noaatidepredictions.html?id=9756639&units=standard&bdate=20141001&edate=20141029&timezone=LST&clock=12hour&datum=MLLW&interval=hilo&action=data

Orth, R.; Carruthers, T.; Dennison, W.; Duarte, C.; Fourqurean, J.; Heck, K.; Hughes, A.; Kendrick, G.; Kenworthy, W.; Olyarnik, S.; Short, F.; Waycott, M., and Williams, S., 2006. A global crisis for seagrass ecosystems. *Bioscience*, 56(12), 987–996.

Otero, E.; Detrés, Y.; Armstrong, A.; Williams, S., and Hernández-López, W., 2014. *Integration of Field, Aerial Photography and Water Quality Measurements for the Assessment of Anthropogenic Impacts and Stressors in Southern Puerto Rico*. Washington, D.C.: National Fish and Wildlife Foundation, *Final Report Submitted to Puerto Rico Seagrass Fund*, 58p.

Pinnel, N., 2007. A Method for Mapping Submerged Macrophytes in Lakes using Hyperspectral Remote Sensing. Munich, Germany: Technical University Munich, Ph.D. dissertation, 164p.

Rodriguez, R.W.; Webb, R.M.T., and Bush, D.M., 1994. Another look at the impact of Hurricane Hugo on the shelf and coastal resources of Puerto Rico, U.S.A. *Journal of Coastal Research*, 10(2), 278–296.

Roelfsema, C.M.; Kovacs, E.; Phinn, S.R.; Lyons, M.; Saunders, M., and Maxwell, P., 2013. Challenges of remote sensing for quantifying changes in large complex seagrass environments. *Estuarine, Coastal, and Shelf Science*, 133, 161–171.

Roelfsema, C.M.; Kovacs, E.; Roos, P.; Terzano, D.; Lyons, M., and Phinn, S., 2018. Use of a semi-automated object-based analysis to map benthic composition, Heron Reef, Southern Great Barrier Reef. *Remote Sensing Letters*, 9(4), 324–333.

Roelfsema, C.M.; Lyons, M.; Kovacs, E.; Maxwell, P.; Saunders, M.; Samper-Villarreal, J., and Phinn, S.R., 2014. Multi-temporal mapping of seagrass cover, species and biomass: A semi-automated object-based image analysis approach. *Remote Sensing of the Environment*, 150, 172–187.

Roelfsema, C.M.; Phinn, S.R.; Udy, N., and Maxwell, P., 2009. An integrated field and remote sensing approach for mapping seagrass cover, Moreton Bay, Australia. *Journal of Spatial Science*, 54(1), 45–62.

Ruiz, H. and Ballantine, D.L., 2004. Occurrence of the seagrass *Halophila stipulacea* in the tropical west Atlantic. *Bulletin of Marine Science*, 75(1), 131–135.

Schowengerdt, R.A., 1983. *Techniques for Image Processing and Classification in Remote Sensing*. Orlando, Florida: Academic Press Inc., 249p.

Short, F.T.; Carruthers, T.J.R.; van Tussenbroek, B., and Zieman, J., 2010. *Thalassia testudinum. The IUCN Red List of Threatened Species 2010*. http://dx.doi.org/10.2305/IUCN.UK.2010-3.RLTS.T173346A6995927.en

Short, F.T. and Wyllie-Echeverria, S., 1996. Natural and human-induced disturbance of seagrasses. *Environmental Conservation*, 23(1), 17–27.

Siermann, J.; Harvey, C.; Morgan, G., and Heege, T., 2014. Satellite derived bathymetry and digital elevation models (DEM). *Proceedings of the International Petroleum Technology Conference* (Kuala Lumpur, Malaysia), pp. 1284–1293.

Tomlinson, P.B., 1974. Vegetative morphology and meristem dependence—The foundation of productivity in seagrasses. *Aquaculture*, 4, 107–130.

Veljanovski, T.; Kanjir, U., and Ostir, K., 2011. Object based image analyses of remote sensing data. *Geodetski Vestnik*, 55(4), 665–688.

Wahidin, N.; Siregar, V.P.; Nababan, B.; Jaya, I., and Wouthuyzen, S., 2015. Object-based image analysis for coral reef benthic habitat mapping with several classification algorithms. *Procedia Environmental Sciences*, 24, 222–227.

Waycott, M.; Duarte, C.M.; Carruthers, T.J.B.; Orth, R.J.; Dennison, W.C.; Olyarnik, S.; Calladine, A.; Fourqurean, J.W.; Heck, K.L.; Hughes, A.R.; Kendrick, G.A.; Kenworthy, W.J.; Short, F.T., and Williams, S.L., 2009. Accelerating loss of seagrasses across the globe threatens coastal ecosystems. *Proceedings National Academy of Science of the United States of America*, 106, 12377–12381.

Williams, S., 1990. Experimental studies of Caribbean seagrass bed development. *Ecological Monographs*, 60(4), 449–469.

Yarbro, L. and Carlson, P., 2015. *Florida Seagrass Integrated Mapping and Monitoring Program Summary Report for Southern Big Bend Region*. SIMM Report #1, pp. 89–95.

Zieman, J.C. and Zieman, R.T., 1989. *The Ecology of the Seagrass Meadows of the West Coast of Florida: A Community Profile*. Washington, D.C.: U.S. Fish Wildlife Service, *Biological Report 85*, 155p.